SAC/EPSA/AESG/ATBD/2024/01

Algorithm Theoretical Basis Document (ATBD) for Particulate Organic Carbon (POC)

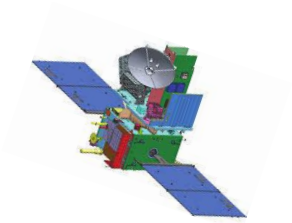

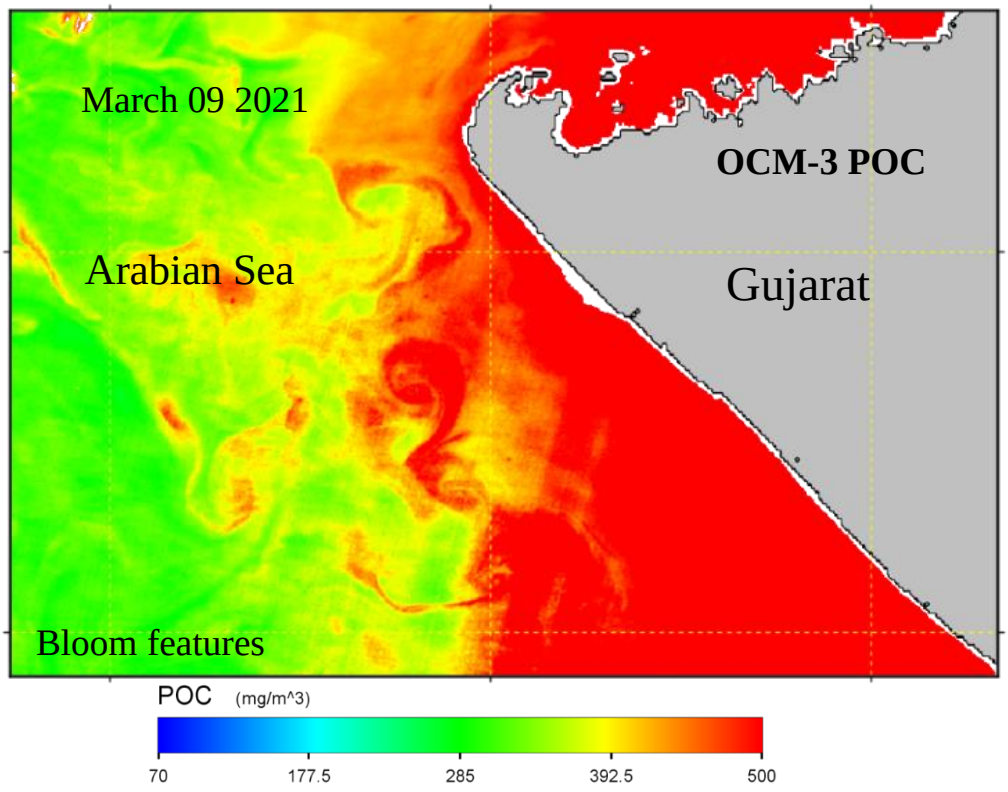

DECEMBER 30, 2024

AESG/EPSA
Space Applications Centre- ISRO, Ahmedabad

Document control sheet

1	Report No.	SAC/EPSA/AESG/ATBD/2024/01
2	Publication Date	December, 2024
3	Title	**Algorithm Theoretical Basis Document (ATBD) for Particulate Organic Carbon (POC)**
4	Type of report	Technical
5	Number of pages	17
6	Authors	R.K.Sarangi, K.Priyanka, B.K.Bhattacharya, K.V.Krishna and P.Shanmugam
7	Originating Unit	AESG/EPSA, SAC
8	Abstract	Estimation of particulate organic carbon (POC) and its space-time variability in global surface ocean waters is essential for understanding the biological export of carbon from the surface to the deep ocean, phytoplankton growth rates, carbon based net primary production and global carbon cycles. The POC concentration in surface waters is highly dynamic and its variability results from various physical and biogeochemical processes. Because of these complex processes the surface ocean POC concentrations vary over a broad range of spatial (regional to global) and temporal (seasonal to decadal) scales. As the POC variations in the surface ocean waters has limitations to solely measure using ships or other in-situ observation platforms. Currently, we have utilized the maximum band ratio index (MBRI) algorithm for POC estimation based on remote sensing reflectance data using 490, 510, 555, 566, 620, 670, 681 nm from EOS-06/Oceansat-3 OCM bands and validated and inter-compared with MODIS-Aqua POC. Regression analysis showed reasonable correlation between *in-situ* and satellite-derived POC concentrations, with OCM-3 (R^2=0.641 & 0.513) data demonstrating better relationships than MODIS-aqua (R^2=0.507 & 0.503) using MBRI and Stramski et al. algorithms. Basing on detailed evaluation and inter-comparison, the ATBD configured for POC product generation using OCM-3 data in northern Indian Ocean region.
9	Keywords	POC algorithm, radiometer data, MBRI, OCM-3, Modis-Aqua, Arabian Sea, Bay of Bengal
10	Security classification	Unrestricted
11	Distribution statement	Among all concerned

Table of content

1. Algorithm Configuration Information

1.1 Algorithm Name: Particulate Organic Carbon (POC) Algorithm

1.2 Algorithm Identifier: E06OCM_POC

1.3 Algorithm Specification Version

Version 1.0 Date: 26/12/2024

Title: POC Algorithm in northern Indian Ocean

Prepared by: Dr. Ranjit Kumar Sarangi, Scientist-SG, AESG/EPSA, SAC

Contributors:

Dr.K.Priyanka, Research Associate, AESG/EPSA, SAC

Dr. Bimal Kumar Bhattacharya, Group Director**,** Scientist-G, AESG/EPSA, SAC

Dr. K.V. Krishna and Dr. P.Shanmugam, IIT- Madras, Chennai

2. Introduction

Ocean plays very important role in linkage to the carbon cycle of the planet earth. There are both the natural and anthropogenic sources which regulate the carbon cycle categorized as sources and sinks. The biological pump is one of the important mechanism for the carbon sequestration to the deep ocean. Phytoplankton, the recognized marine primary producers utilize new and recycled nutrients to convert the dissolved inorganic carbon to particulate organic carbon (POC) (Eppley and Peterson, 1979; Longhurst and Harrison, 1989). A fraction of POC is then exported vertically to deep waters by various mechanisms (downwelling, detrainment, etc), as consumption by zooplankton and fish, excretion of faecal pellets and by particle aggregation and sinking. Understanding the fate of POC is crucial as it influences carbon sequestration, atmospheric CO_2 levels and global climate patterns. POC, produced by marine biotic components such as phytoplankton through photosynthesis, sinks from the surface to the deep ocean and sediments, serving as a major pathway for carbon sequestration (Kharbush et al., 2020; Wu et al., 2023). The transport of POC from distant sources and its varied characteristics, such as particle size, enhance its role in oceanic biogeochemistry and optical properties (Dall'Olmo et al. 2009; Kings et al. 2017; Stramski et al. 2022).

2.1. Overview and Background

Particulate Organic Carbon (POC) in the ocean is a crucial component of the global carbon cycle, affecting both biological processes and carbon fluxes. POC includes non-living organic detritus, heterotrophic organisms, and phytoplankton (Parsons et al. 1984; Kharbush et al. 2020), playing a vital role in the oceanic ecosystem. It is key to the biological export of carbon from surface waters to the deep ocean and serves as food for marine organisms (Volk and Hoffert, 1985; Ducklow et al. 2001). Through the "biological pump," POC is exported to deeper layers or recycled through the microbial loop, influencing dissolved organic and inorganic carbon pools (Volk and Hoffert, 1985; Ducklow et al. 2001). Despite its small size, POC has high turnover rates due to its diverse components like phytoplankton, bacteria, zooplankton, and organic detritus, contributing significantly to oceanic fluxes (Gardner et al. 2006; Stramska, 2009).

The rate at which POC degrades, affected by factors like temperature, microbial activity, and depth of re-mineralization, determines how effectively carbon is stored in sediments versus released back into the atmosphere by Kandasamy et al. (2019). POC concentrations vary spatially and temporally, influenced by biological productivity, water temperature, and nutrient availability, with higher productivity regions typically showing elevated POC levels (Lima et al., 2014). Recognizing these dynamics is essential for accurately assessing the ocean's role in the global carbon cycle and its impact on climate change.

As the EOS-06 mission extends with Oceansat-2 bridging to Oceansat-3, it is timely to refine global POC algorithms using remote sensing reflectance, Rrs(λ) data from multiple satellite datasets. POC is a key product in the Global Ocean Carbon Observation System, poised for exploitation and utilization. Global validation and selection of the best algorithm are crucial (CEOS, 2014). In a recent study on POC algorithms using satellite-field matchups, King et al. (2017) examined performance. Ocean colour products are influenced by various sources of errors, arising from factors such as choice of sensor, calibration procedures, and atmospheric correction methods used to retrieve Rrs(λ) data (Kings et al. 2017). Additionally, when POC algorithms rely on inherent optical properties (IOPs), the methods used to derive these products from Rrs(λ) data introduce further considerations. Given the significance of Rrs(λ) as an input parameter for estimating surface ocean POC, it becomes imperative to validate satellite-derived Rrs(λ) data against in-situ measurements. While verification efforts initially focused on IOPs like particulate backscattering coefficient (bbp) and particle beam attenuation coefficient (cp), attention has changed towards validating absorption coefficients due to their crucial role in ocean colour remote sensing.

In this document, two different globally developed algorithms were employed: one by Stramski et al. 2008, which utilizes blue-to-green band ratios (bands at 443 and 555 nm), and another by Krishna et al. 2023, analysing green–red–near-infrared bands (maximum band ratio index (MBRI) approach) with slightly reduced accuracy in blue bands. These algorithms are utilized to estimate POC concentrations in the ocean using satellite data. To validate the algorithms, Rrs(λ) from Moderate Resolution Imaging Spectro-radiometer (MODIS)-Aqua data and Ocean Colour Monitor-3 (OCM-3) data are compared with in-situ data in the Arabian Sea (AS) region. POC algorithms applied to new satellite launches, such as OCM-3 Rrs(λ), mark a significant milestone in oceanographic research and monitoring.

The study presents a comprehensive validation in Arabian Sea using in-situ Rrs data sets along with OCM-3 satellite-derived Rrs. And this method is essential to provide a common reference data for comparison between sensors, which can be useful for merging satellite data into climatological records. In addition, assessment of the performance and accuracy of POC algorithms needed by comparing their results with in-situ data from the northern Indian Ocean region.

2.2. Objectives

- Demonstrate the adaptation of global POC algorithm to satellite mission EOS-06 Oceansat-3/OCM-3 data.
- Comparison of empirical POC algorithms
- Evaluation of POC output from OCM-3 Rrs with respect to global products

2.3. Input data sets

2.3.1. Satellite data

Global empirical algorithm developed by using 488, 510, 547, 555, 645, 667, 678nm bands in MODIS data remote sensing reflectance and validated with in-situ datasets. Similar close-by input bands are

available in Oceansat-3 OCM sensor 490, 510, 555, 566, 620, 670, 681 nm. Hence, the in situ based inter-comparison carried out with both satellite outputs and the statistical results evaluated. The outcomes are useful for Oceansat-3 (OCM-3) mission, science application program. The Level-2c Rrs data both LAC and GAC is accessed having 360m and 1Km resolution. The algorithm's performance will be refined with inputting more in situ cruise data points over different regions, different depth waters and seasons, as future focus.

2.3.2. In-situ Remote sensing reflectance (Rrs) data

Optical data (remote sensing reflectance) was collected using Satlantic hyperspectral underwater radiometer (Sahay et al. 2019; Verma et al., 2021; Sarangi et al., 2023) in the AS coastal waters (Figure 1). The depth of all station points were within 15–200 m and highly optically complex in terms of chemical and biological components. The radiometer operates in 256 channels covering the wavelength range of 350–800 nm with sampling rate of 3.3 nm/pixel. The Prosoft software module (version-7.7.16) of Satlantic HyperPro was used in computing remote sensing reflectance. It works with three sensors to measure upwelling radiance (Lu), downwelling irradiance (Ed), and surface downwelling irradiance (Es). Sunlight interacts with water particles, leading to absorption and reflection. After setting up the equipment, the radiometer was deployed at the station (Fig. 1) for measurements, which were repeated with three casts and stored in a data logger connected to a PC and average of the three casts data stored and plotted for Rrs finally. This procedure was followed at all stations, with water samples collected for quality POC analysis. The observed surface remote sensing reflectance (Rrs) was estimated from water-leaving radiance ($L_w(0^+,\lambda)$) and downwelling irradiance ($E_d(0^+,\lambda)$) (Mobley, 1994).

$$Rrs = \frac{L_w(0^+,\lambda)}{E_d(0^+,\lambda)} \quad (1)$$

Where,

$$L_w(0^+,\lambda) = L_u(\lambda)\left(1 - \frac{\rho_r(\lambda)}{\eta_w^2(\lambda)}\right) \quad (2)$$

$$E_d(0^+,\lambda) = \frac{E_d(\lambda)}{1-\alpha} \quad (3)$$

In equations 1-3, α, ρ_r, and η^2_w are the Fresnel reflection albedo from sun and sky (0.043), reflectance index of seawater (0.021), and refractive index of seawater (1.345), respectively. This has been considered as per the radiometer data analysis software (Prosoft 7.7 Product Manual 2017) for calculation of water leaving radiance, L_w and this radiometer derived data used in several research wok on development of ocean colour algorithms and applications using in situ data (Chauhan et al. 2002; Sarangi et al. 2008). The significant ocean colour component is R_{rs} which is defined as the ratio of upwelling spectral radiance to the downwelling spectral irradiance and measured in per steradian. R_{rs} and L_w are crucial parameters in determining the water types and useful in the algorithm development for the estimation of particle concentration from the biogeochemical sources. Measurements were performed under clear sky conditions, relatively low sun zenith angles and relatively calm sea state with stable platform (Tilstone et al., 2020, Dev and Shanmugam 2016 & 2017; Sahay et al. 2019; Sarangi et al., 2008, 2022 & 2023). Matchups between satellite observations and ship-based stations locations were retrieved for 2 × 2 pixel windows co-located with observations of image acquisition followed.

3. Algorithm functional specification

3.1. Theoretical background on the Empirical algorithm implementation

3.1.1. Spectral reflectance based MBRI approach

The estimation of surface ocean POC concentration using spectral remote sensing reflectance (Rrs(λ)) involves the utilization of various combinations of spectral bands. These combinations are derived from remote sensing data collected by satellites and provide valuable information for quantifying POC concentrations in the ocean (Krishna et al, 2023). Figure 1 offers a comprehensive visual representation of the Rrs(λ) spectral signature curves, capturing the distinctive properties displayed by diverse oceanic water types. These curves provide valuable insights into the unique characteristics and optical behaviour exhibited by different water types present in the ocean and coastal zones. By analysing these spectral signatures, one can gain a thorough and visually enhanced understanding of the reflectance variations across different wavelengths in the visible and NIR spectrum.

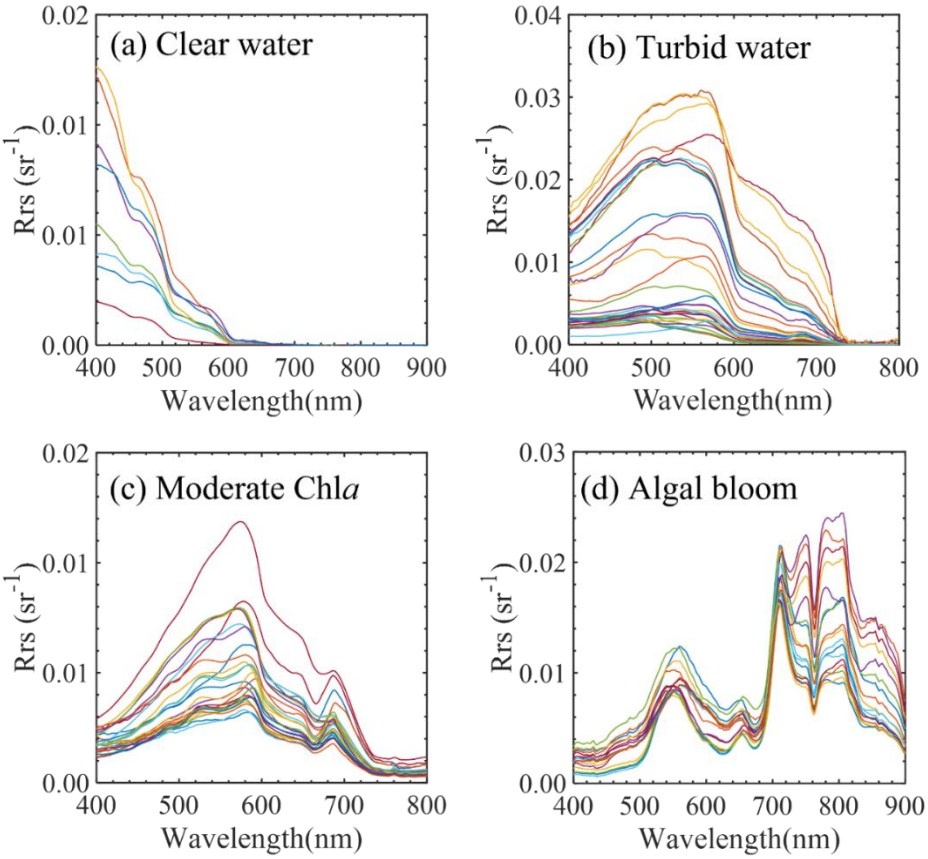

Figure 1: Spectral signature curves of different oceanic water types with distinctive characteristics. The in-situ data for (a) clear water (Atlantic Ocean, N=8), (b) turbid water (Yellow Sea, N=34), and (c) moderate Chl-a (Chesapeake Bay, N=26) were obtained from the SeaBASS website, while data for (d) algal bloom water types (N=17) were obtained by OOIL team in Mutthukadu lagoon water (Singh et al., 2019; Singh and Shanmugam, 2016; Varunan and Shanmugam, 2017)

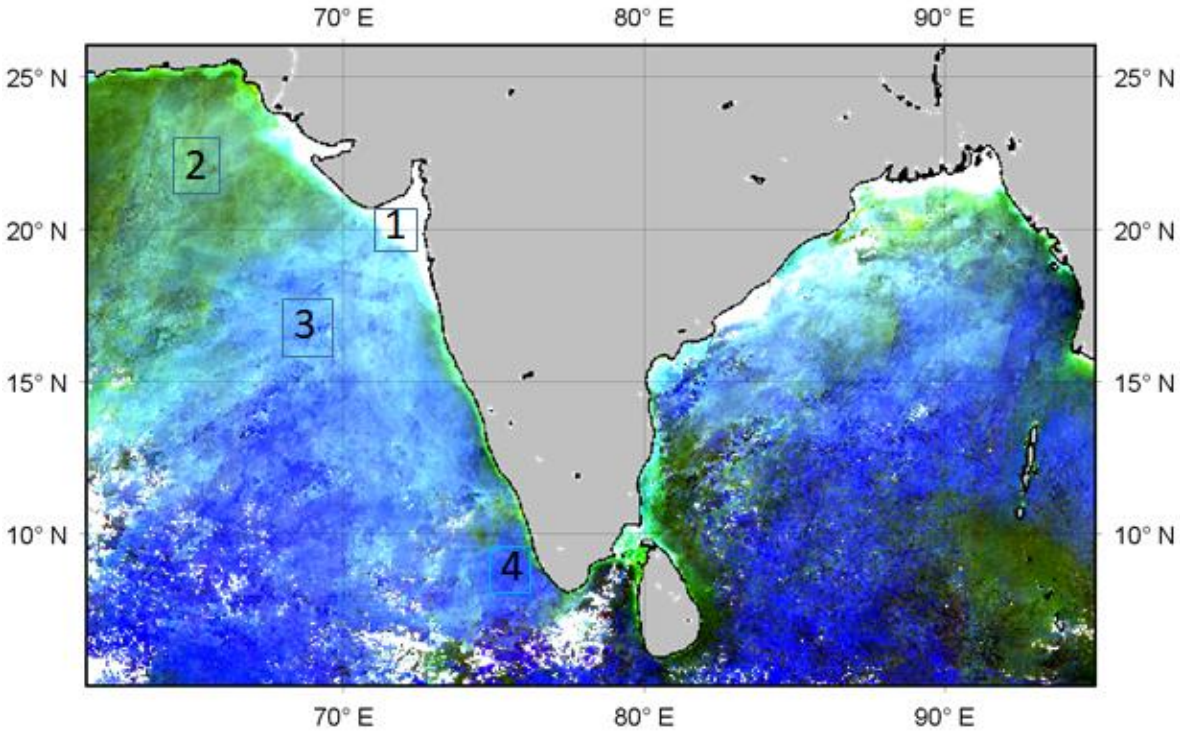

Figure.2. Natural colour composite image from OCM-3 in the northern Indian Ocean during December, 2023, showing (1) sediment laden water, (2) High chlorophyll bloom type water, (3) Moderate chlorophyll water, (4) Low chlorophyll water types.

In recent years, multiple spectral band ratio approaches have been developed and become popular for different oceanic regions. In most of the global ocean water types (Fig. 1 a-c)), the blue to green band ratio algorithms (Joshi et al., 2023; Liu et al., 2015; Stramska, 2009; Stramski et al., 2022; Woźniak et al., 2016) are widely used to estimate surface ocean POC concentrations. The blue to green band ratios provides valuable insights into the spatial distribution and temporal variability of POC concentrations in the global oceans. However, in extremely rare cases such as highly productive algal bloom waters, (Fig. 4(d)) red to green band ratio play predominant role as compared to blue to green band ratio (spectral Rrs(λ) at red band is more dominant than blue band) to estimate the POC concentration (Tran et al., 2019). These areas exhibit extreme physical and biogeochemical conditions, including significant variations in phytoplankton composition and the presence of mineral-dominated particles. The red to green band ratio become more relevant in such regions due to their sensitivity to specific pigments and mineral content, providing insights into the specialized POC dynamics occurring in these regions. In addition, the red to green band ratio is influenced by the phenomenon of chlorophyll fluorescence which occurs when chlorophyll molecules re-emit the absorbed light energy, usually in the red region of the spectrum (Gower et al., 1999; Xing et al., 2007). This fluorescence signal can be detected by remote sensing instruments and is related to the presence and activity of living phytoplankton. The detailed information of red to green band ratios used for the estimation of POC concentration in coastal waters are presented in the Tran et al. (Tran et al., 2019) MBR approach.

3.1.2. MBRI model formulations

The spatiotemporal variability of POC in oceanic waters is largely controlled by the complex physical (physical mixing), biological (phytoplankton production and biological pump) and chemical processes (remineralization). These processes are often studied based on the respective water constituents, IOPs

and AOPs. The POC estimates from the water constituents' concentrations and IOPs may be associated with the significant uncertainties (Le et al., 2018). To overcome this uncertainty, multiple approaches have been developed based on the spectral band ratios (Hu et al., 2016; Liu et al., 2015; Stramski et al., 2022), band differences (Le et al., 2018), and reflectance based approaches (Le et al., 2017). The spectral reflectance band ratio is the most popular among other approaches to estimate the spatiotemporal variability of large scale POC concentrations (Allison et al., 2010; King et al., 2017; Stramski et al., 2008). In recent years, multiple spectral band ratio approaches have become popular for different oceanic regions such as open ocean waters (Stramska, 2009), river-dominated waters (Le et al., 2017; Liu et al., 2015), highly turbid and productive waters within coastal and inland environments (Liu et al., 2015; Tran et al., 2019). These band ratio approaches work reasonably well in the regions where in-situ data were collected for model development and validation purposes and inadequate for global scale applicability. The global POC from OCM-3 data is generated using MBRI approach and shown in Figure-3.

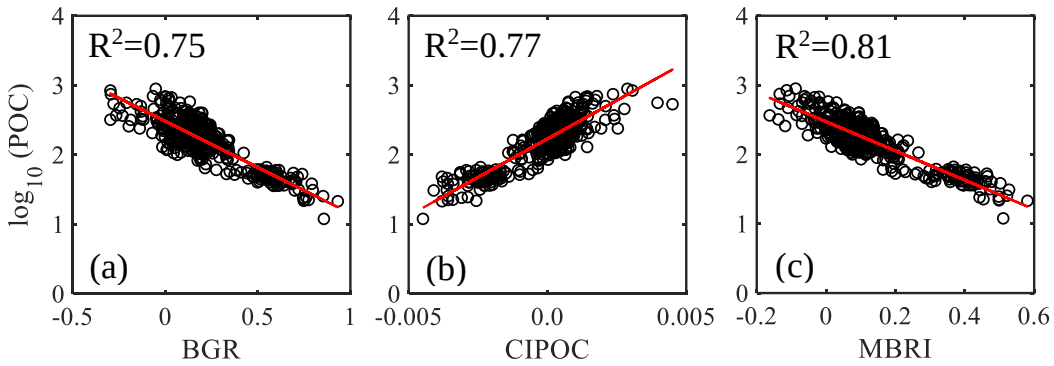

Fig. 3. The parametrization plots of the relationships (logarithmic scale) between (a) POC and global BGR approach (Rrs (443): Rrs (555)), (b) POC and global CIPOC approach, (c) POC and present MBRI approach (N=441). The values of the squared correlation coefficient (R2) are also provided for comparison purpose.

Thus, our empirical formulations of the present MBRI approach were derived using Rrs(λ) data at 488, 531,547,555, 645, 667 and 678 nm as follows

$$\text{Avg} = \text{Average}(\text{Rrs}(510), \text{Rrs}(555), \text{Rrs}(566)) \quad \text{---------- (4)}$$

$$\text{MBRI} = \log_{10}\left(\text{Maximum}\left(\frac{\text{Rrs}(490)}{\text{Avg}}, \frac{\text{Rrs}(620)}{\text{Avg}}, \frac{\text{Rrs}(670)}{\text{Avg}}, \frac{\text{Rrs}(681)}{\text{Avg}}\right)\right) \quad \text{----------(5)}$$

where the maximum band ratio index (MBRI) is the log transformed ratio of the blue (488nm) and red (645, 667 and 678nm) bands to the average values of the green (531, 547 and 555nm) bands. Figure 7(c) shows the relationship of in-situ POC versus concurrent satellite-derived MBRI data. Similar algorithm parameter and coefficients were derived from the in-situ POC and coincident satellite-derived BGR (Figure 7(a)) and CIPOC (Figure 7(b)) using the same dataset. Figure 8 indicates that MBRI produced a high correlation (R2=0.81) compared to the existing BGR (R2=0.75) and CIPOC (R2=0.77) indexes. This indicates the effectiveness and robustness of MBRI for producing the surface ocean POC estimations. Thus, the MBRI index values were used to establish an empirical formulation of the present MBRI approach, which is given by

$$POC = 10^{A(MBRI)+B} \quad \text{----------(6)}$$

In this equation, both A and B are coefficients that are to be fitted, and MBRI is the ratio of the maximum of blue and red bands to the average of green bands. The best fit regression coefficients for the MBRI approach are given as

$$POC = 10^{(-2.1081*MBRI+2.4725)} \quad \text{----------(7)}$$

The MBRI algorithm has the capability to generate POC global maps at different spatial scales (such as basin and global) and temporal resolutions (including daily, monthly, seasonal, and annual) across various latitudes, longitudes, and ocean basins. In addition, the MBRI approach can be applied to other ocean/water colour sensors over the regional and global ocean waters.

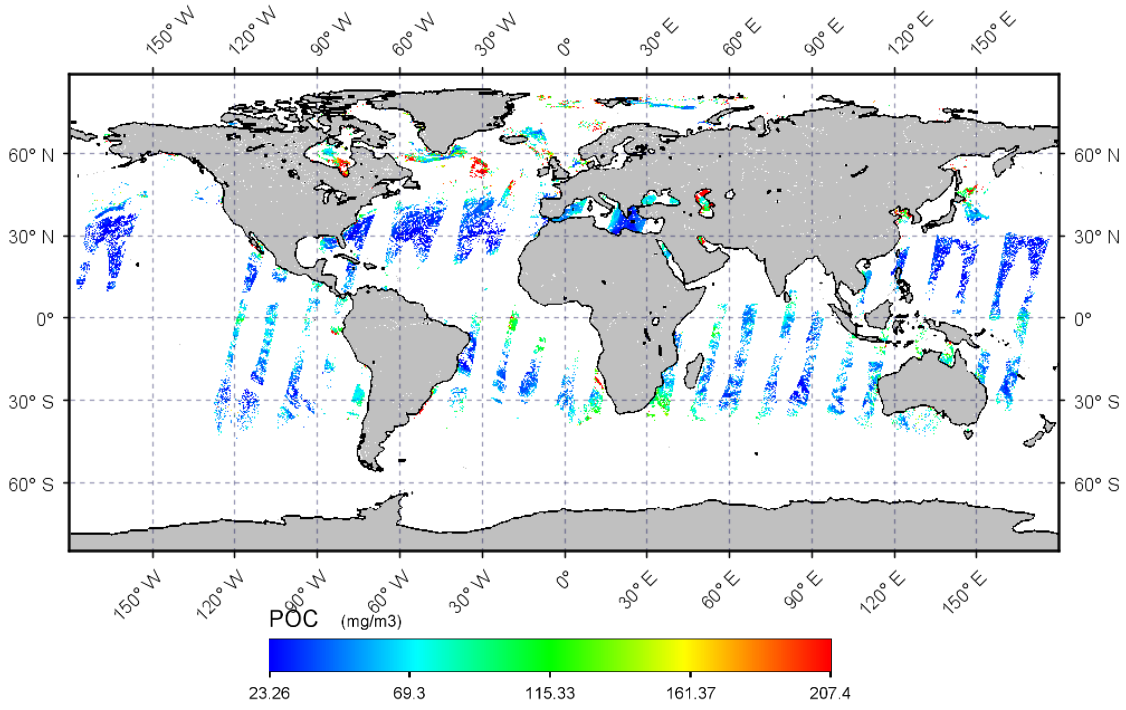

Fig.4. The global surface ocean on 30th June 2023 one day image POC concentrations derived from the MBRI approach using OCM-3 GAC.

3.2 Steps for Operational implementation

Step 1: Access to OCM-3 LAC/GAC Rrs data from the Bhoonidhi NRSC site.
Step 2: Data quality check on the availability of cloud-free or less cloudy OCM-3 Rrs data from Bhoonidhi.
Step 3: Integrate the Rrs data into the POC algorithm.
Step 4: Evaluate and analyze POC concentrations, which range from 50 to 500 mg/m^3.
Step 5: To generate daily, 3-days, 8-days and monthly composite data

4. Evaluation of POC algorithm

4.1. In situ radiometer and Remote sensing observations

Stramski et al. (2008) developed a POC empirical algorithm based on power-law between near-surface POC and blue-to-green ratio. They use remote-sensing reflectance at Rrs(λ) 443 and Rrs(λ) 555 to derive the POC algorithm. The empirical algorithm of Stramski et al. (2008) based on the power function of the blue-green reflectance ratio has been used by NASA for routine determinations of global POC product from past and current satellite ocean colour missions. Krishna et al. (2023) developed a POC algorithm using a simple maximum band ratio index (MBRI) approach based on global POC and Rrs data. They utilized a combination of specific Rrs bands (Rrs(λ) 488, Rrs(λ) 531, Rrs(λ) 547, Rrs(λ) 555, Rrs(λ) 645, Rrs(λ) 667, Rrs(λ) 678) to derive the algorithm. However, for application in the AS using OCM-3 satellite data, adjustments were made using nearby Rrs. The OCM-3 sensor provides Rrs data in different bands (Rrs(λ) 490, Rrs(λ) 510, Rrs(λ) 555, Rrs(λ) 566, Rrs(λ) 620, Rrs(λ) 670, Rrs(λ) 681). These adjustments ensured the algorithm's suitability for the OCM Rrs(λ).

The empirical algorithm of (Stramski et al. 2008) were based on Rrs(λ) data at 490 and 555.

$$POC = 203.2 * \left(\frac{Rrs\ 490}{Rrs\ 555}\right)^{-1.034} \text{----------(8)}$$

The empirical formulations of (Krishna et al 2023) MBRI approach were based on Rrs(λ) data is as follows:

Avg = Average (Rrs(λ)(510), Rrs(λ)(555), Rrs(λ)(566))----------(9)

$$MBRI = \log_{10}\left(Maximum\left(\frac{Rrs\ 490}{Avg}, \frac{Rrs620}{Avg}, \frac{Rrs670}{Avg}, \frac{Rrs681}{Avg}\right)\right) \text{----------(10)}$$

$$POC = 10^{(-2.1081*MBRI*2.4725)} \text{----------(11)}$$

The power-law (equation 4) and MBRI POC algorithm (equations 5 to 7) effectively generate POC maps across various spatial scales, from basin to global levels, and temporal resolutions, typically monthly. The MBRI approach, when applied to OCM-3 data, is particularly suitable for assessing POC dynamics in the AS, providing insights into the distribution and variations of particulate organic carbon in this region.

4.2. Steps: Flow chart of POC Product generation

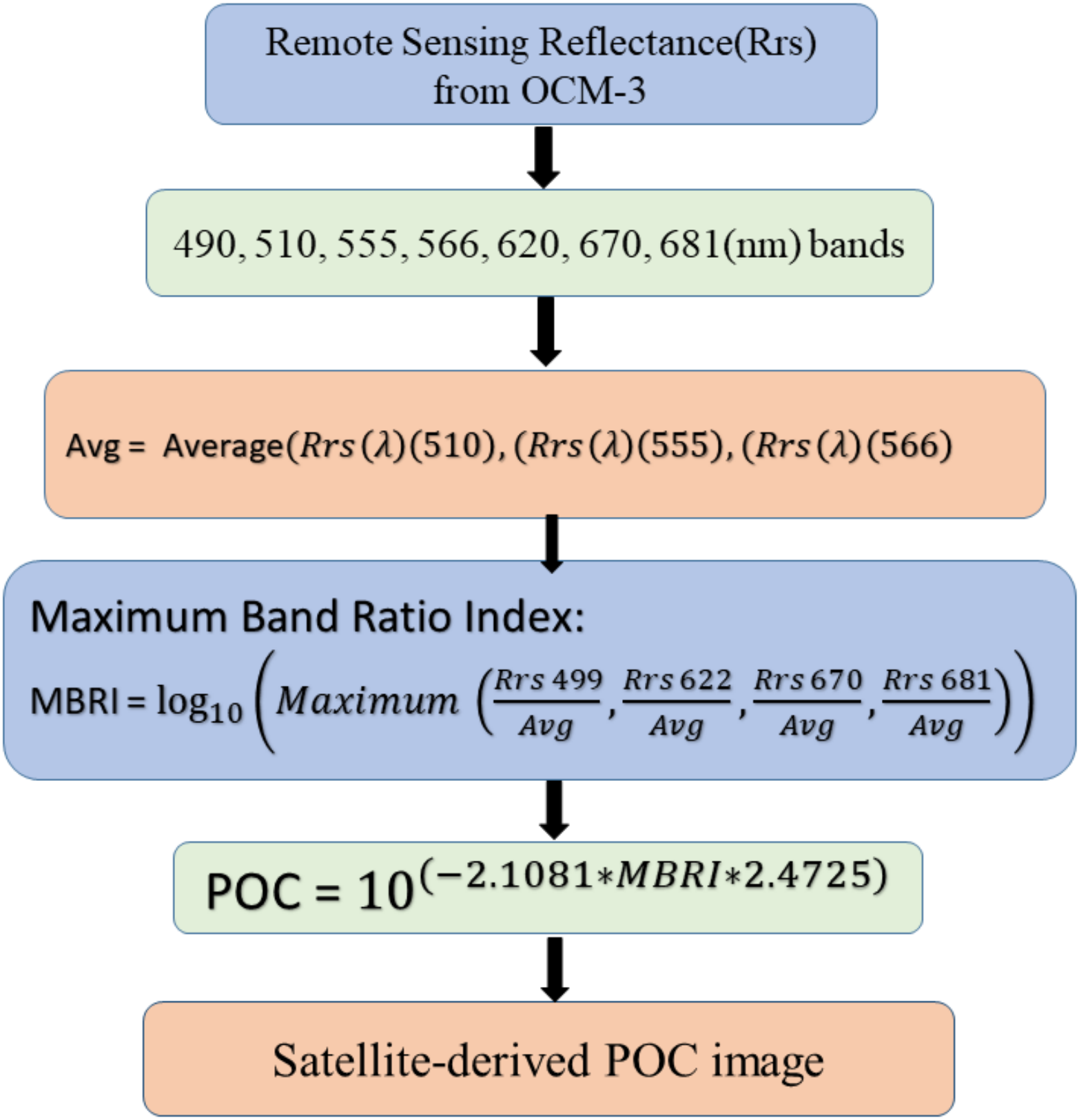

Figure. 5. A flow chart showing the POC algorithm and its steps.

4.3. Validation of in-situ Rrs (λ) and satellite retrieved Rrs (λ) OCM-3 and MODIS-Aqua Rrs

Fig.6.The map showing a) total 63-stations on board Sagar Tara cruise (054/2024) in coastal AS, b) southern coastal, c) central coastal d) northern coastal regions, used for in situ and satellite data validation.

4.3.1 Comparisons of *in-situ* Rrs (λ) and satellite retrieved Rrs (λ) from OCM-3 and MODIS-Aqua data

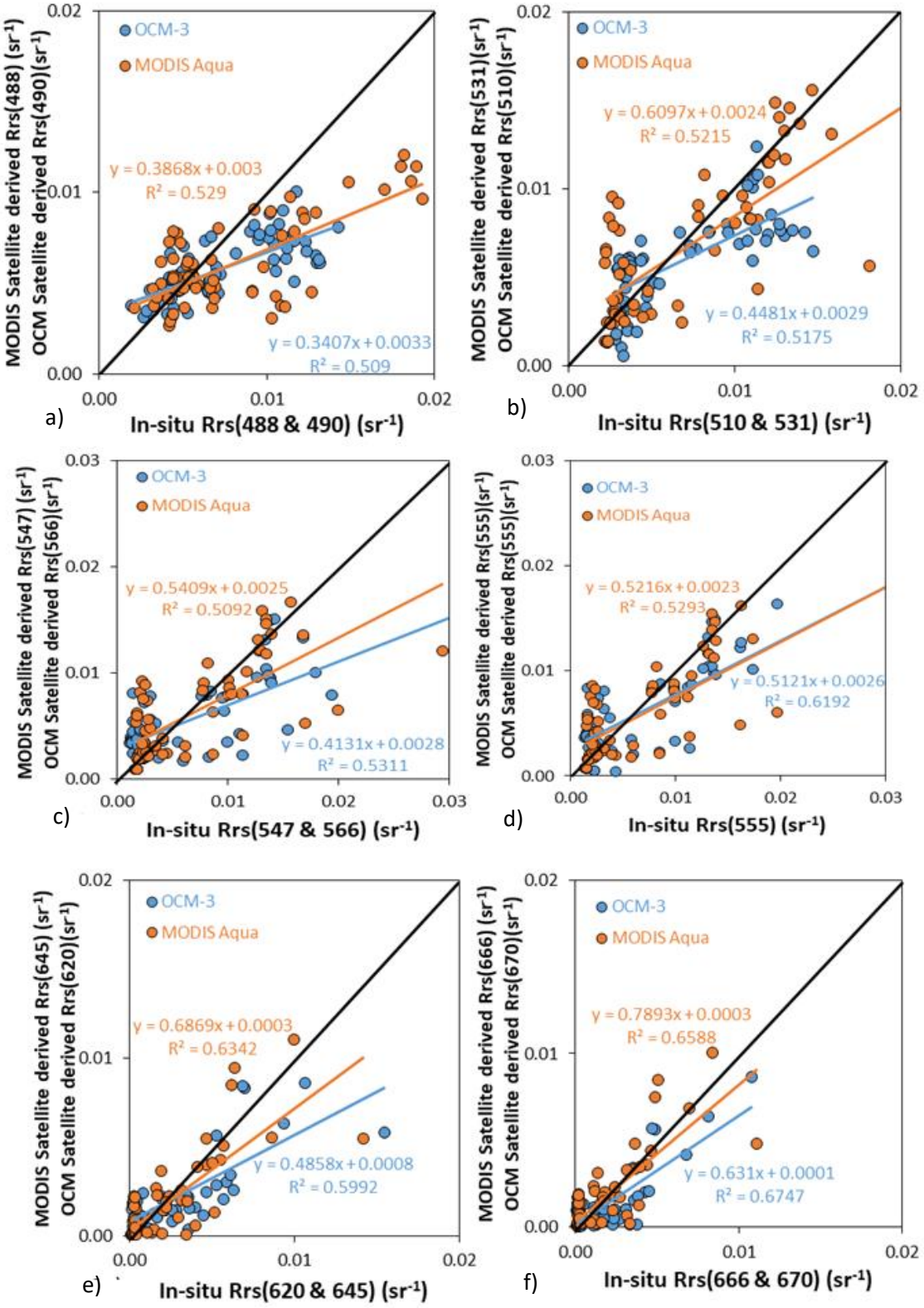

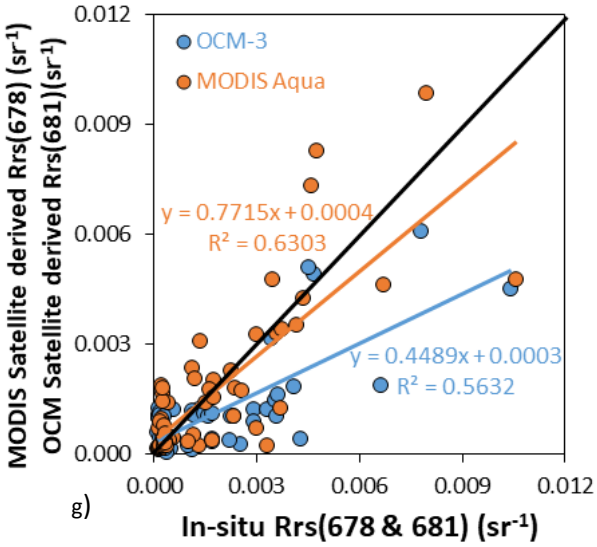

Fig.7. Scatterplots of the *in-situ* Rrs (λ) and satellite retrieved Rrs (λ) from OCM-3 and MODIS-Aqua data blue bands (a) Rrs 488 and 490, green bands (b) Rrs 510 and 531, (c) Rrs 547 and 566, (d) Rrs 555, red bands (e) Rrs 620 and 645, (f) Rrs 666 and 670, (g) Rrs 678 and 681 (number of observations, N= 63).

5. Output

5.1 Format of output

The output format (netcdf or geotif) and generated POC map will be hosted on the MOSDAC Web platform.

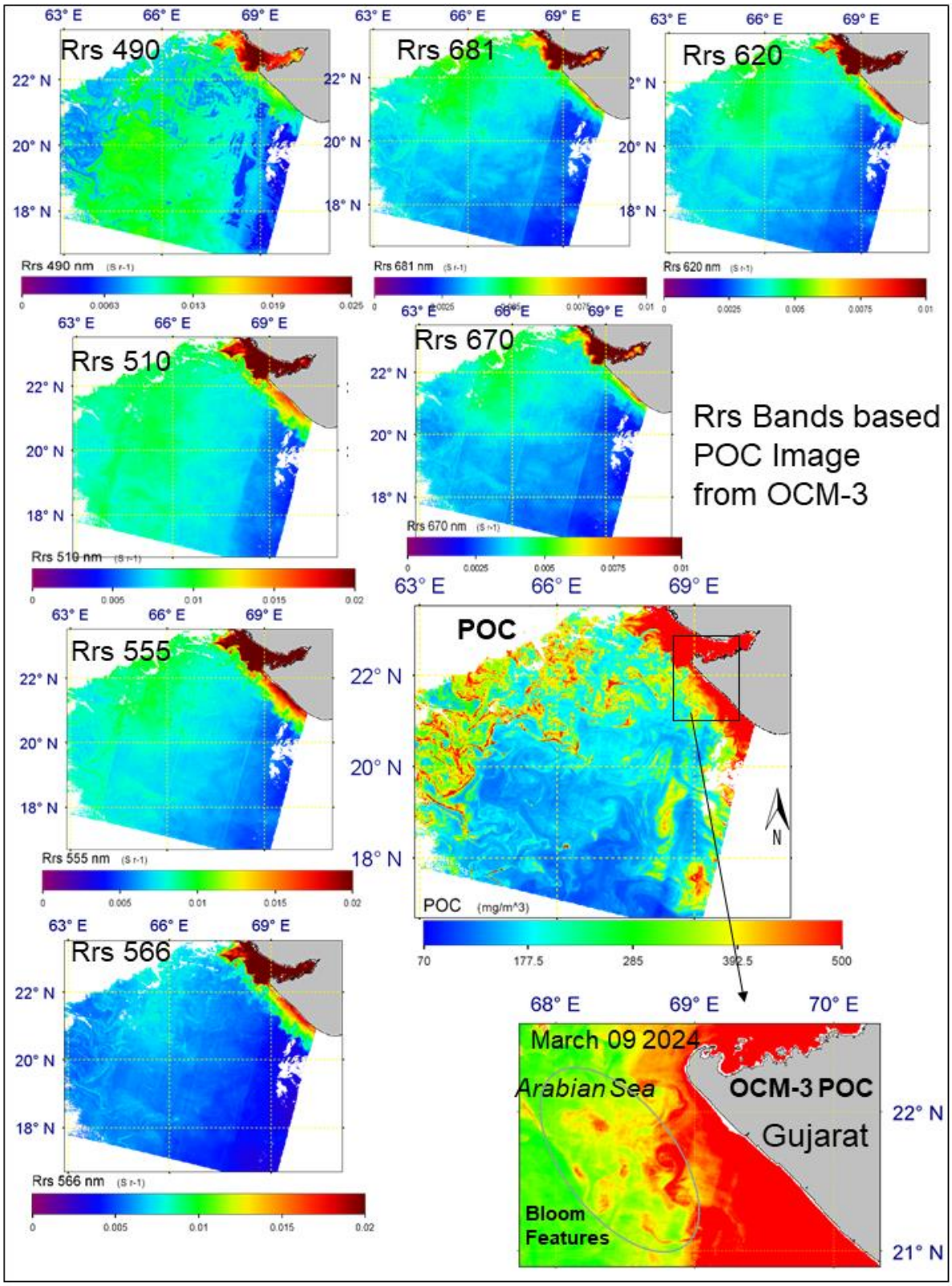

Figure 8. MBRI approach based satellite-derived POC using OCM-3 Rrs data

5.2. Generation of OCM-3 derived Rrs and POC product using LAC

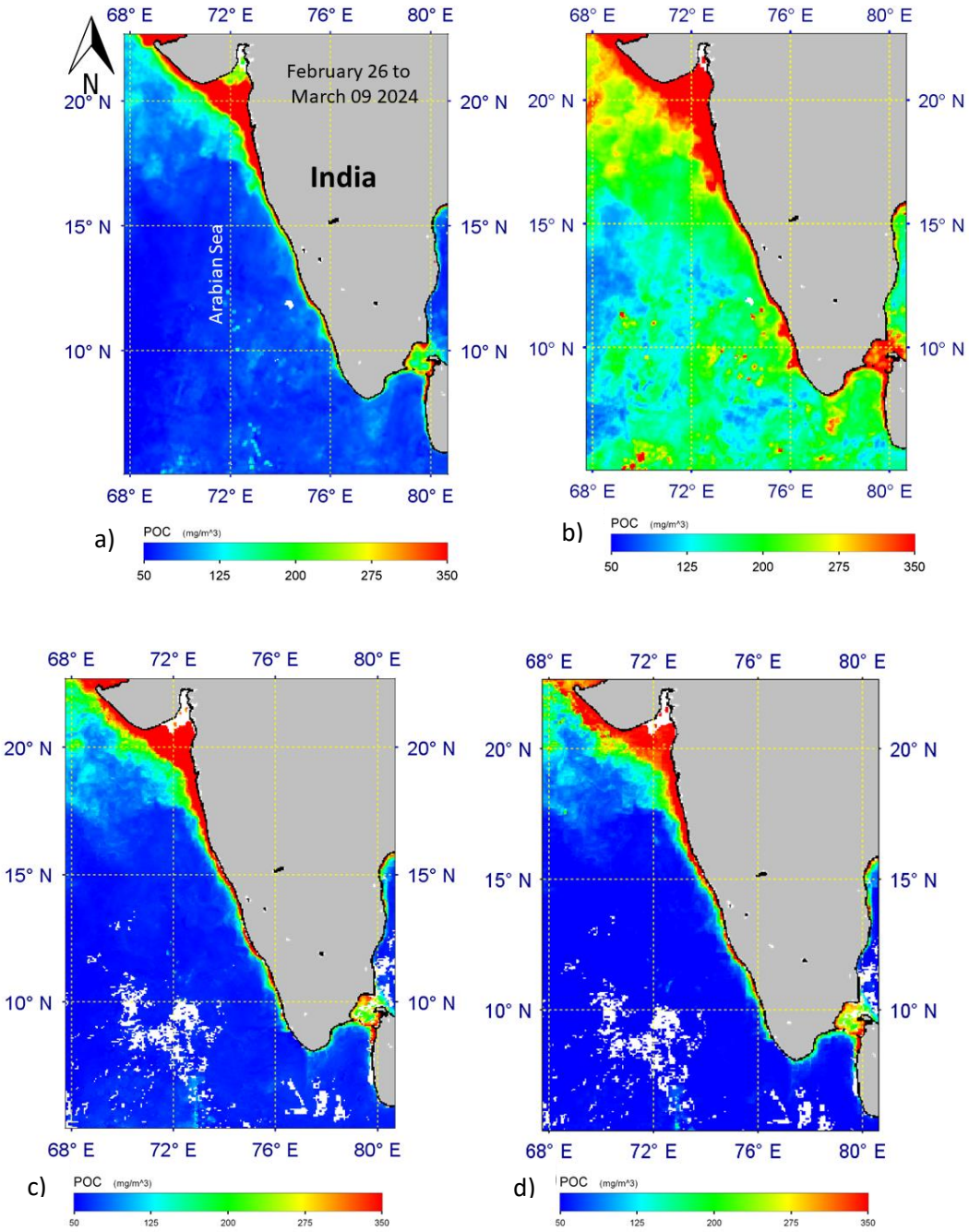

Fig.9 Surface POC product derived from OCM-3 using a) MBRI approach by Krishna et al. 2023, b) power law function approach by Stramski et al. 2008, similarly POC product derived from MODIS using c) MBRI approach by Krishna et al. 2023 and d) power law function approach by Stramski et al. 2008.

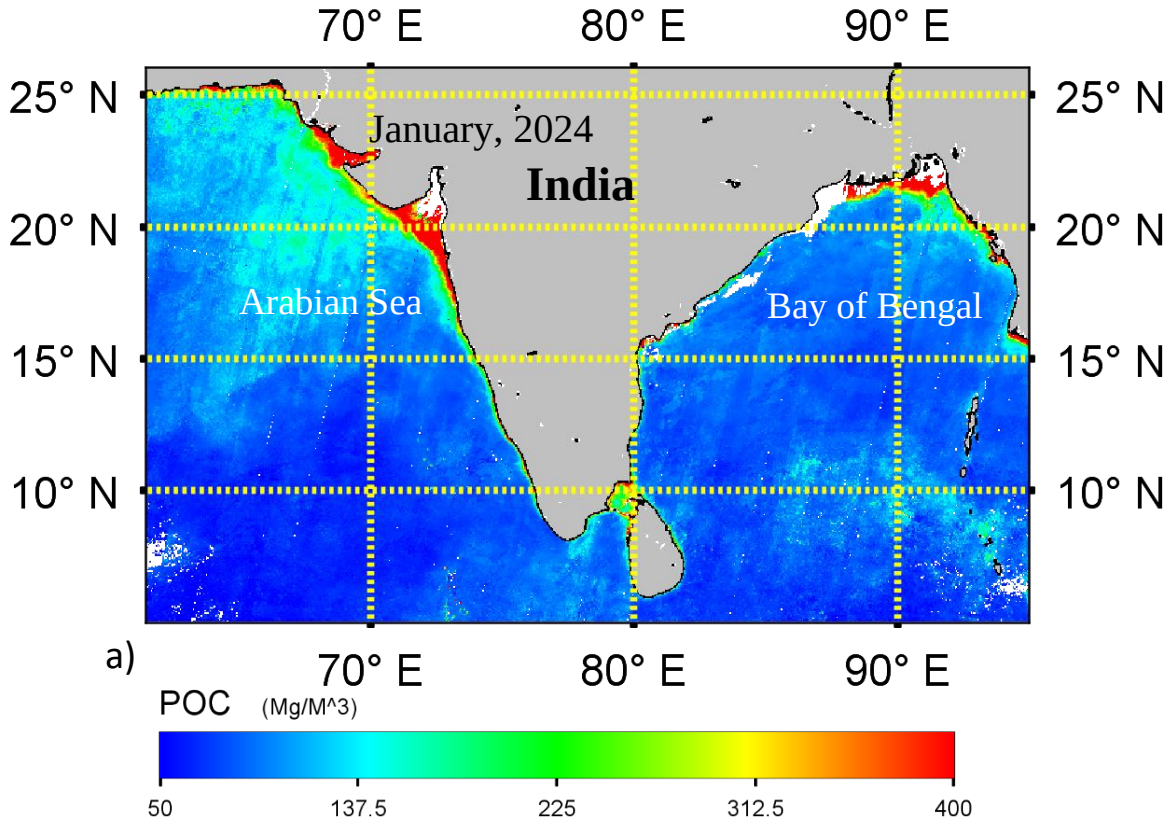
70° E
80° E
90° E
25° N
20° N
15° N
10° N
January, 2024
India
Arabian Sea
Bay of Bengal
a)
POC (Mg/M^3)
50
137.5
225
312.5
400

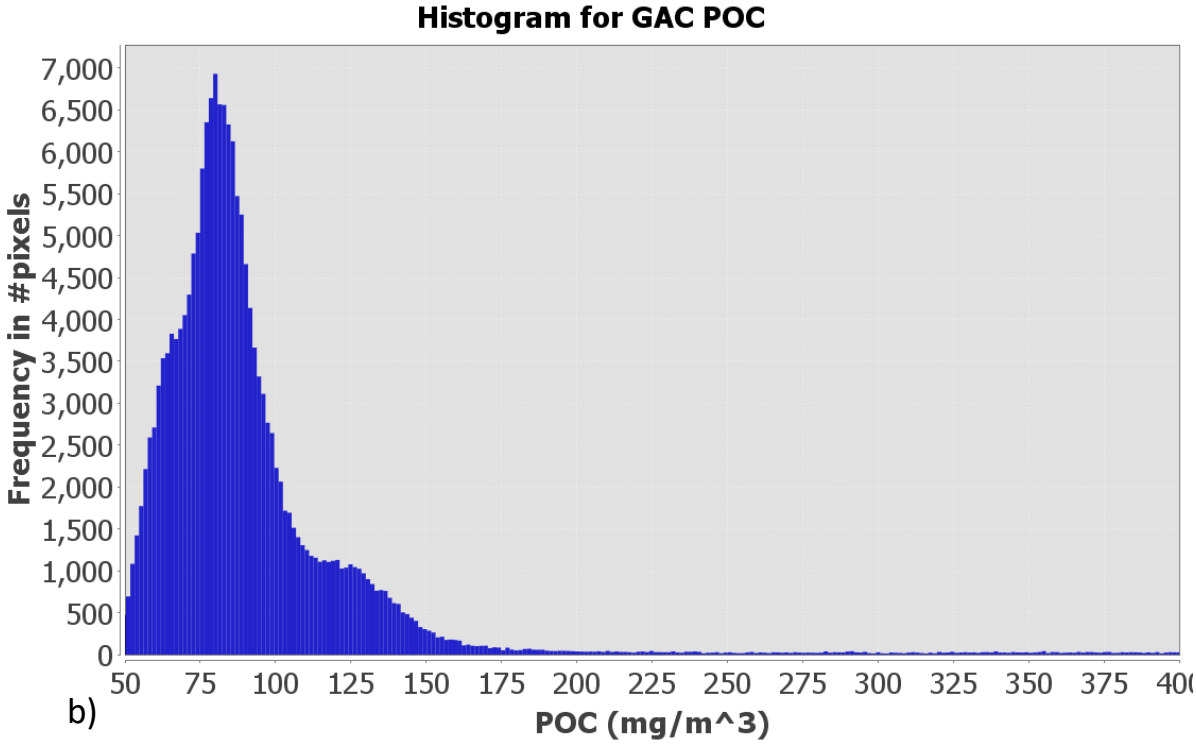
Histogram for GAC POC
Frequency in #pixels
7,000
6,500
6,000
5,500
5,000
4,500
4,000
3,500
3,000
2,500
2,000
1,500
1,000
500
0
50
75
100
125
150
175
200
225
250
275
300
325
350
375
400
POC (mg/m^3)
b)

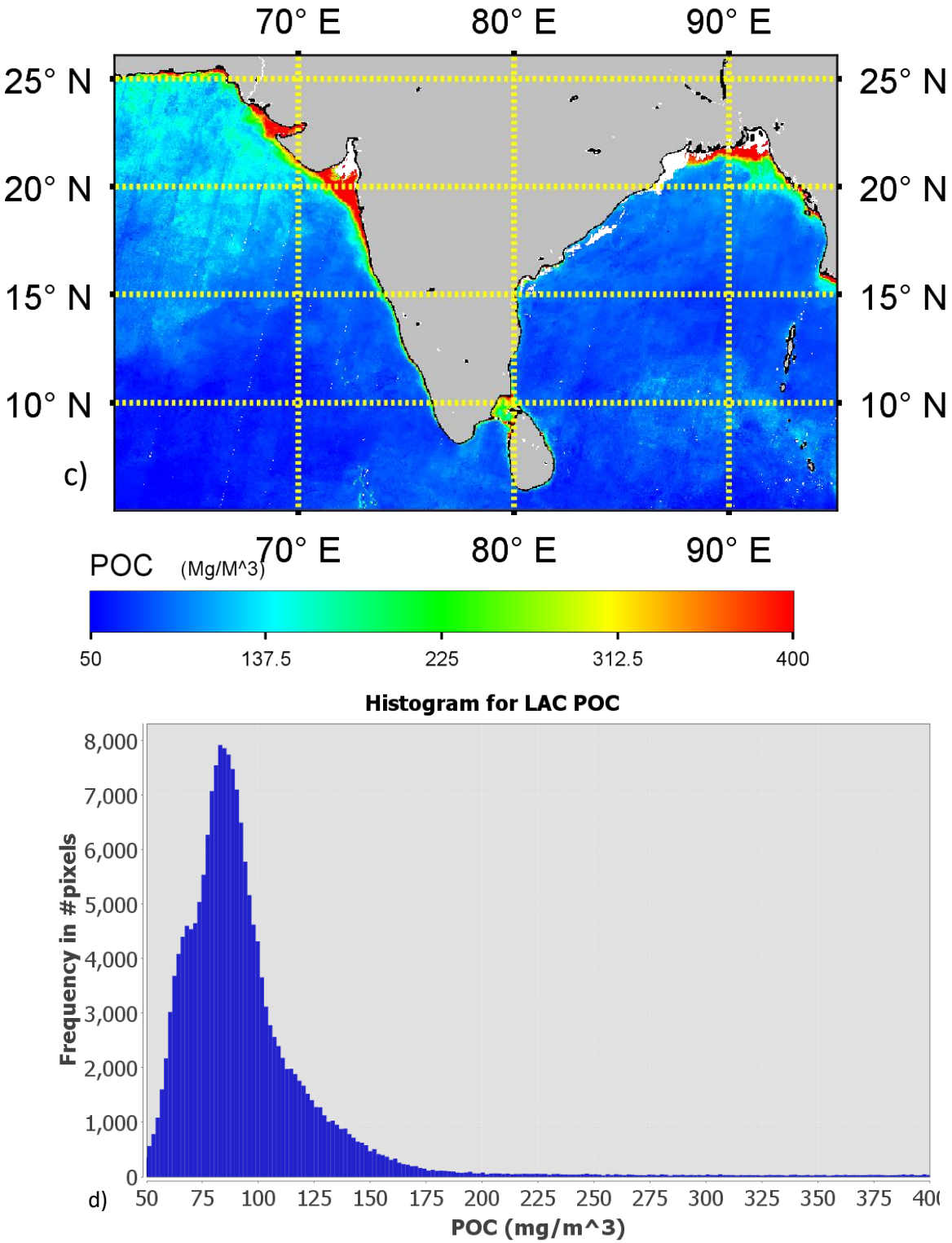

Fig.10. The POC concentrations derived from the MBRI approach using a) OCM-3 GAC b) Histogram-GAC c) OCM-3 LAC d) histogram-LAC in the northern Indian Ocean monthly image on December 2023.

5.3. Inter-comparison of POC algorithm

Ocm-3 and MODIS-Aqua Products

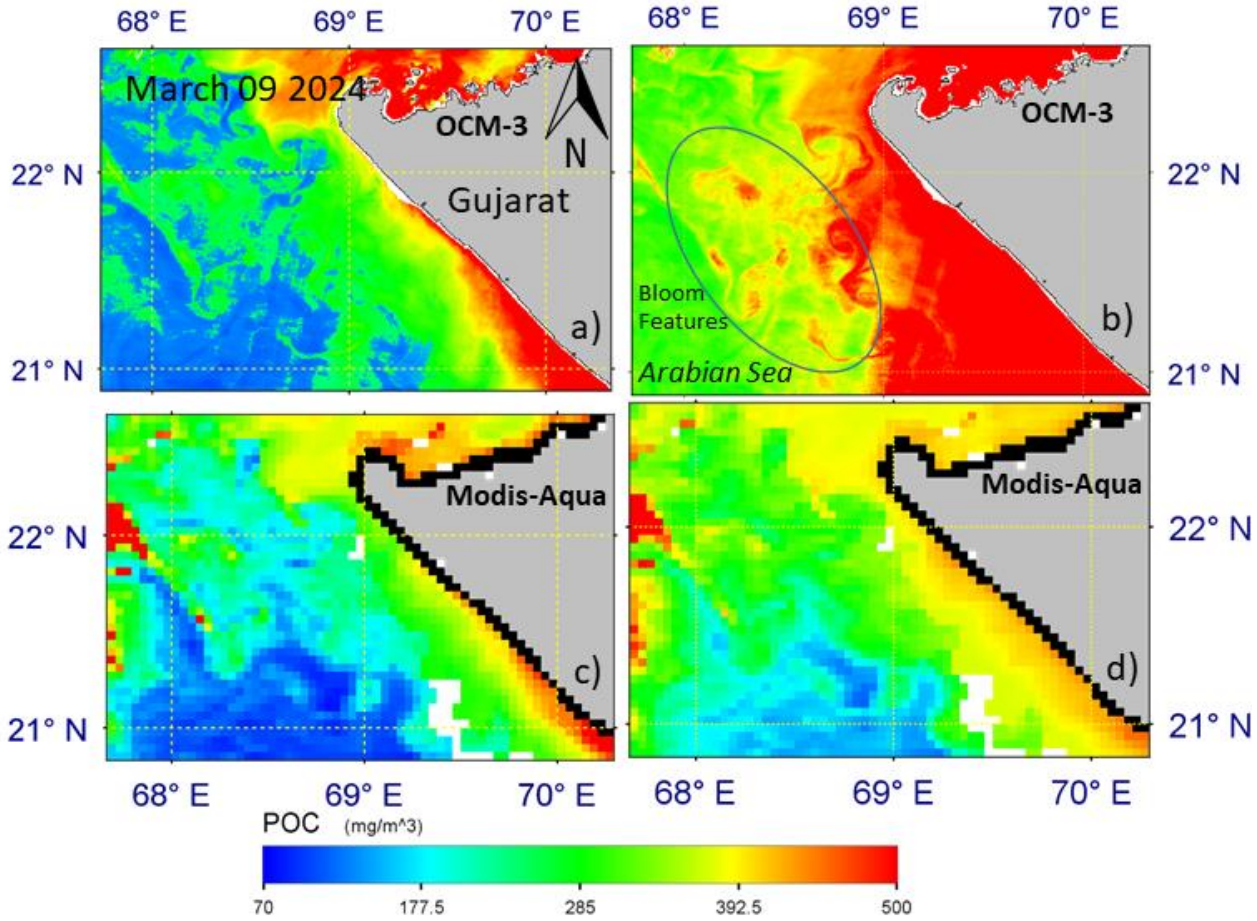

Fig. 11. Surface POC product derived from OCM-3 using a) MBRI approach by Krishna et al. 2023 b) power law function approach by Stramski et al. 2008 and MODIS using c) MBRI approach by Krishna et al. 2023 d) power law function approach by Stramski et al. 2008.

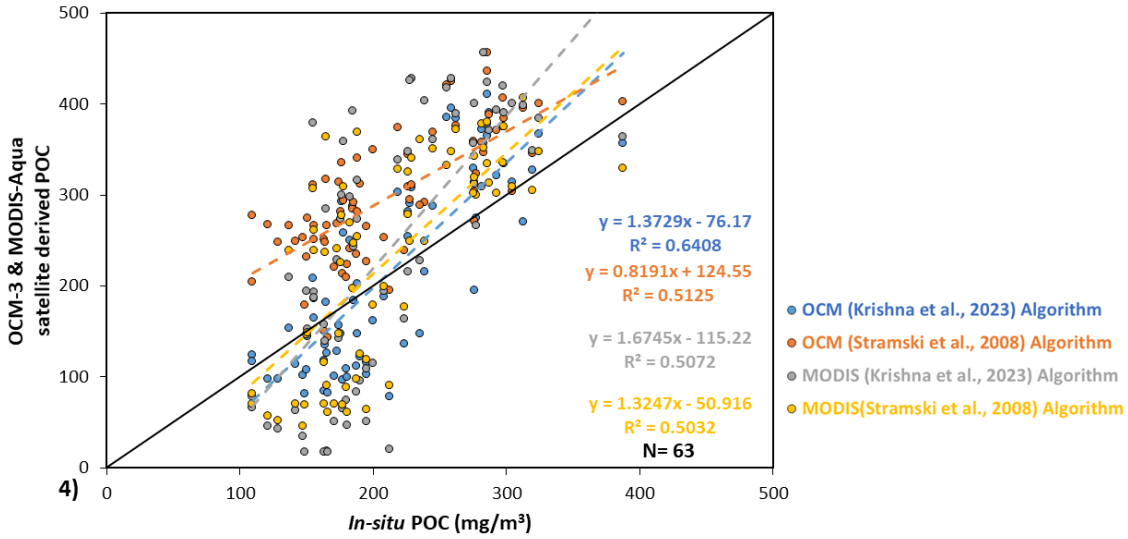

Fig.12. Inter-comparisons and regression analysis of *in-situ* and satellite-derived POC of OCM- 3 and MODIS-Aqua, black line indicating 1:1 plot.

Table-1 Statistical results show the MBRI algorithm performance

Sensors	Distinct algorithm	Number of points	In-situ range (mg/m³)	Satellite range (mg/m³)	R^2	MAE (mg/m³)	RMSE (± mg/m³)	MRD (mg/m³)	MNB (mg/m³)
OCM-3	Stramski et al.,	63	109 to 387	114 to 588	0.513	-1.758	146.794	63.14	21.3
	Krishna et al.,			78 to 589	0.641	-0.335	100.53	34.63	23.1
Modis Aqua	Stramski et al.,			70 to 570	0.503	-0.446	109.49	55.80	46.5
	Krishna et al.,			56 to 568	0.507	-0.674	134.23	46.20	30.8

5.4. Linkage with PFZ locations

In the Gujarat coastal region, POC and chlorophyll ranged from 135 to 442 mg/m3 and 0.88 to 2.87 mg/m3 respectively (fig.13 a & b). In the southeast Kerala region, POC and chlorophyll ranged from 48 to 241 mg/m3 and 0.31 to 1.82 mg/m3 respectively (fig.14 a & b). Chlorophyll-a and POC shows the significant relationship of R2=0.97. This suggests that an important portion of the POC is composed of marine diatoms, dinoflagellates and/or brown algae which contain chlorophyll-a. Particulate Organic Carbon, POC, and Chlorophyll-a, Chl-a, are key indicators for identifying Potential Fishing Zones, (PFZ), as they reflect marine productivity and fish availability. POC represents organic matter from phytoplankton and detritus, while Chl-a indicates phytoplankton biomass, the foundation of the marine food web. High concentrations of both suggest nutrient-rich waters that attract zooplankton and fish, commonly found in upwelling zones, river discharge regions, and oceanic fronts. Satellite enhances PFZ prediction, aiding sustainable fisheries management and optimizing fishing efforts.

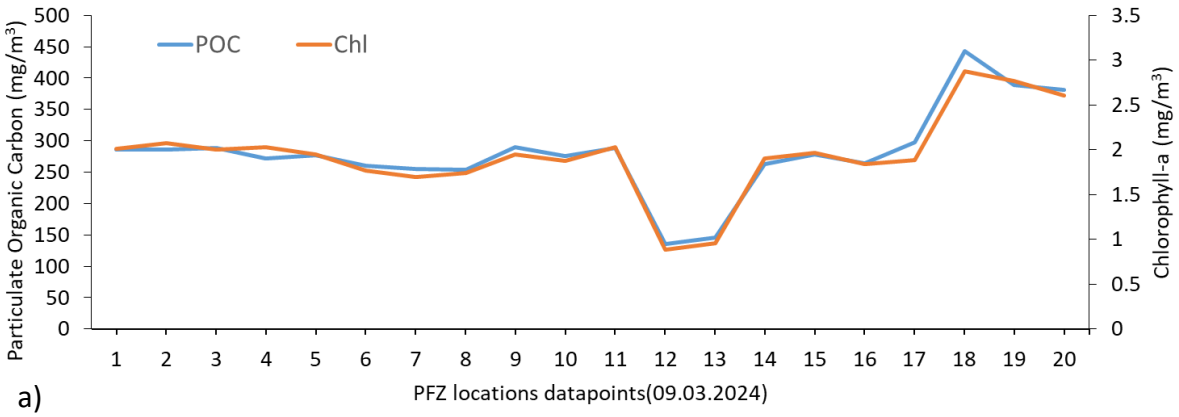

a)

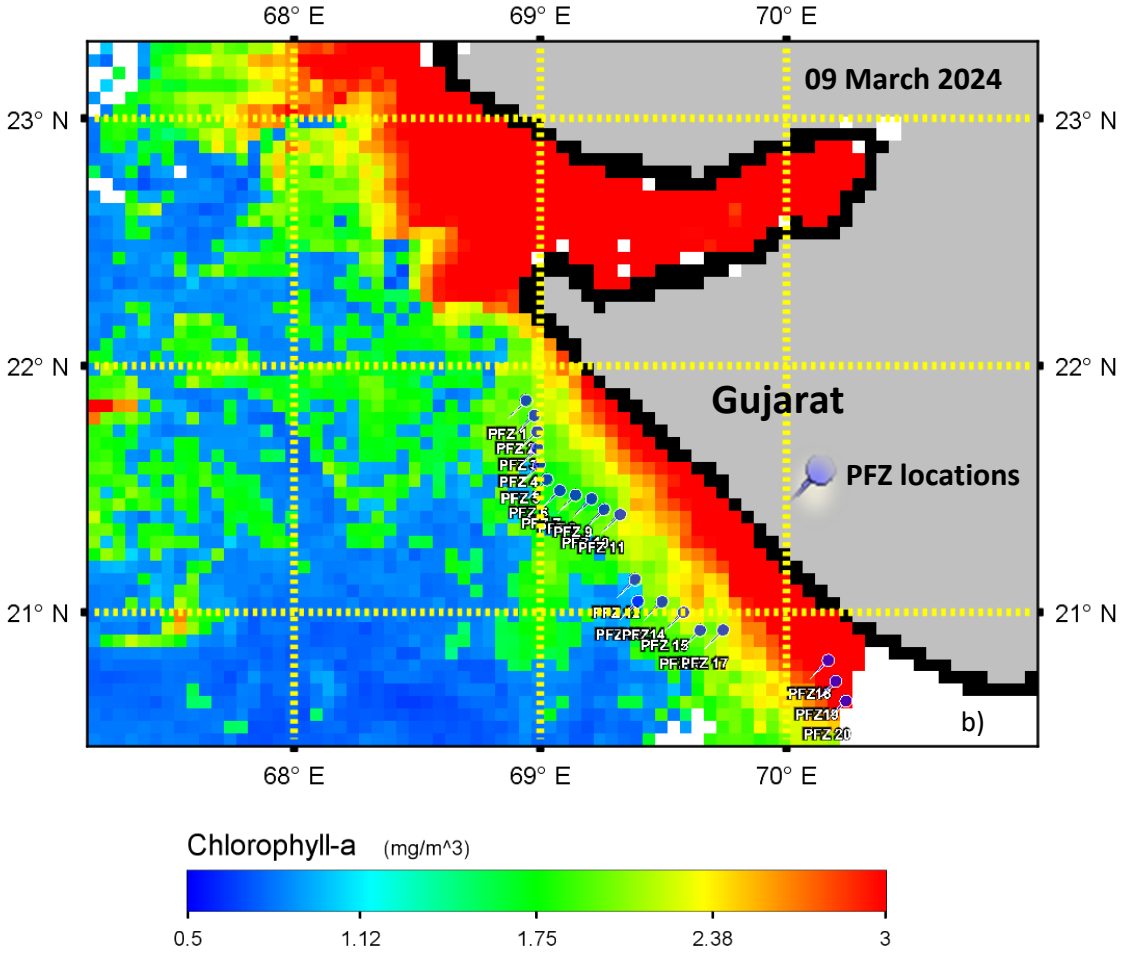

Fig. 13. a) Variation of particulate organic carbon and chlorophyll in the PFZ zone location b) OCM-3 derived chlorophyll image and pins indicate the PFZ zone during 09 march 2024.

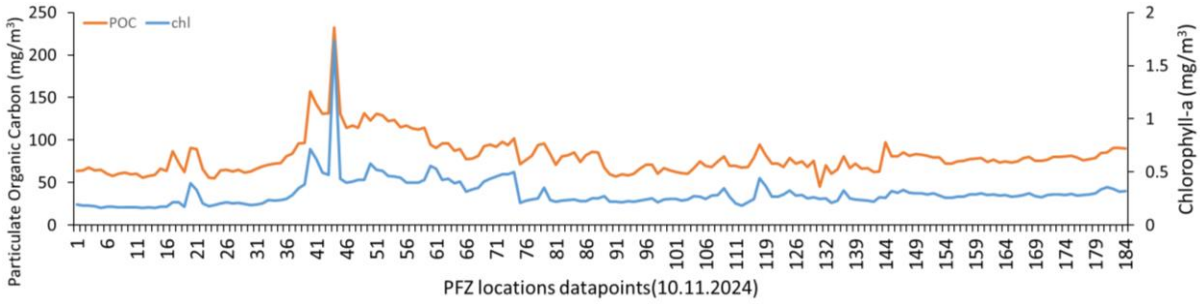

a)

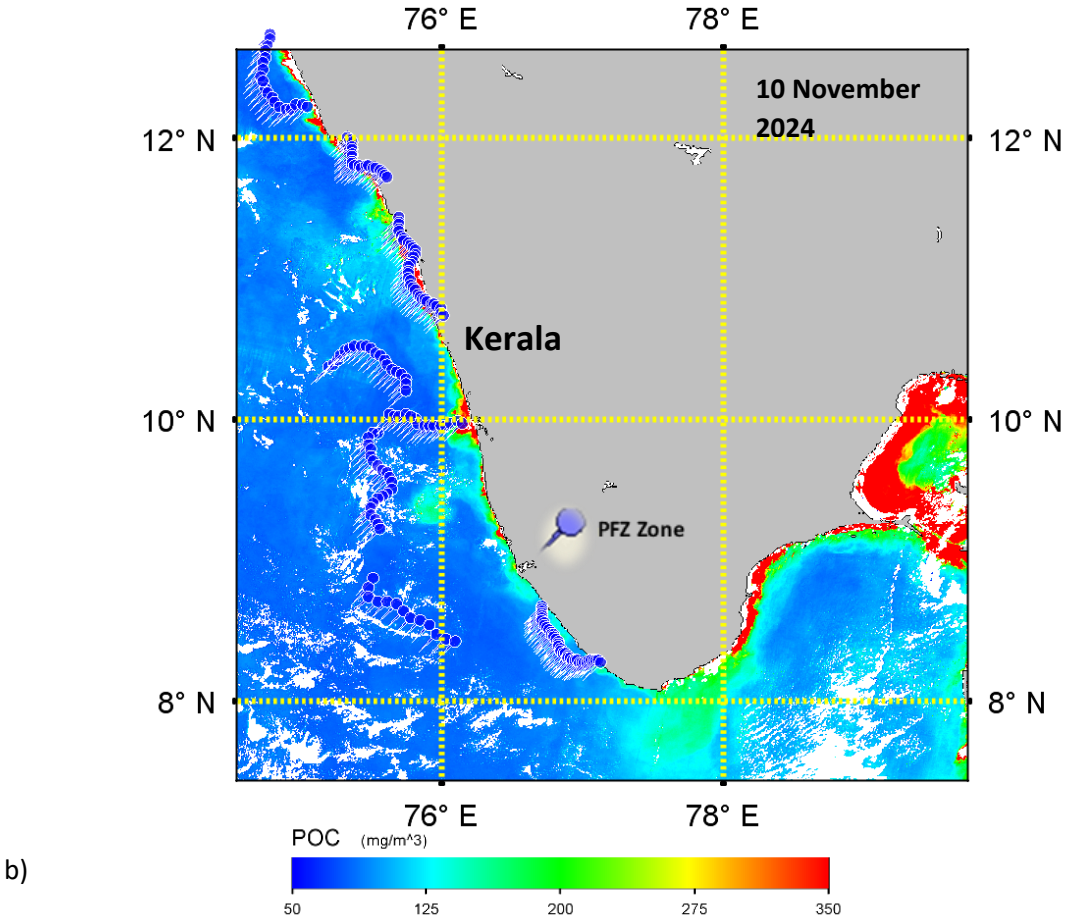

Fig. 14. a) Variation of particulate organic carbon and chlorophyll in the PFZ zone location b) OCM-3 derived chlorophyll image and pins indicate the PFZ zone during 10 November 2024.

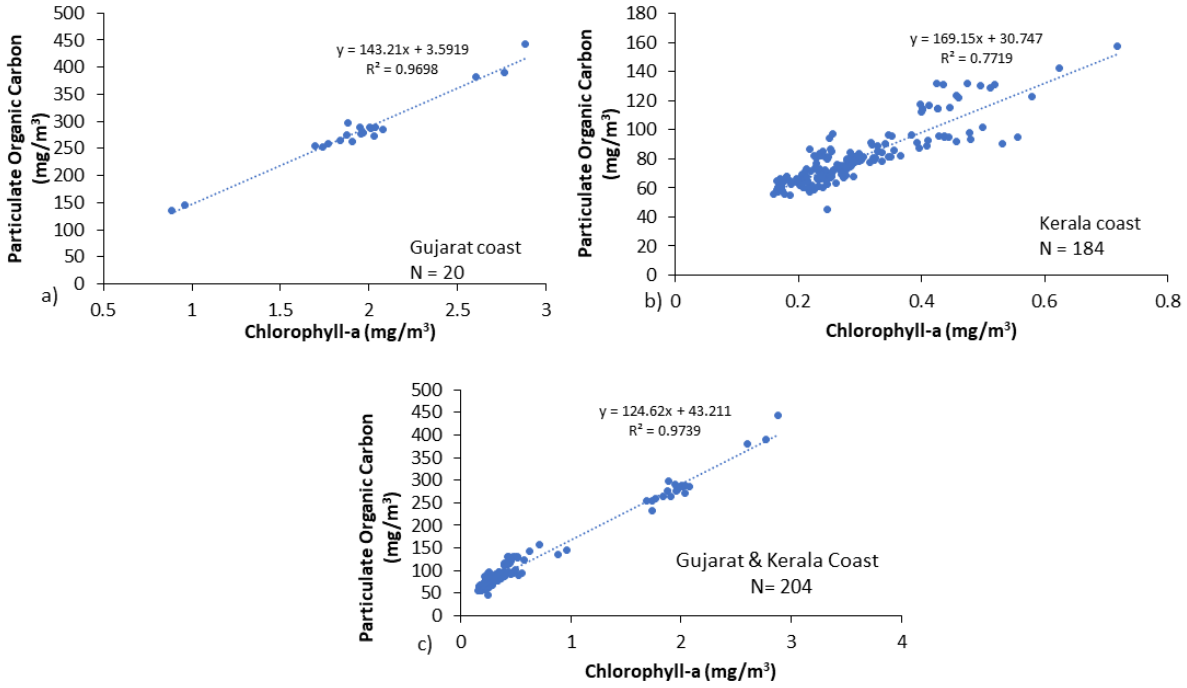

Fig.15. Regression analysis of Chlorophyll and POC a) Gujarat coast (09.03.2014) b) Kerala coast (10.11.2024) C) both Gujarat and Kerala in the PFZ zone

5.5. Global distribution of POC observed from OCM-3 and MODIS-Aqua sensor.

The distribution of Particulate Organic Carbon (POC) observed from OCM-3 and MODIS-Aqua spans the Atlantic Ocean, Pacific Ocean, Southern Indian Ocean, and Southern Ocean (fig.16). Globally, POC concentrations vary from 10 to 900 mg/m³, with notable differences between coastal and offshore regions. Coastal areas exhibit higher productivity compared to offshore regions, indicating greater biological activity near the shore. The OCM-3 sensor demonstrates a strong correlation with POC estimates from the well-established MODIS-Aqua satellite, highlighting its reliability in assessing oceanic carbon dynamics.

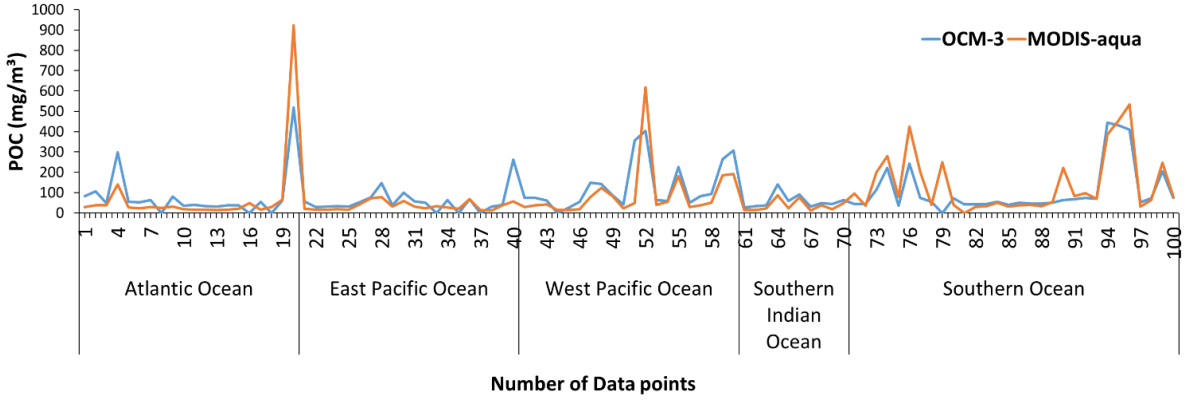

Fig. 16.Global distribution of POC observed from OCM-3 and MODIS-Aqua sensor

The comparison was made using the OCM-3 GAC and MODIS-Aqua POC products to evaluate the POC values trend across different regions (fig.15). Due to non-availability of in situ Rrs and in situ POC data over other oceans in recent time frame, the actual comparison with respect to OCM-3 sensor derived POC couldn't be evaluated over other global ocean regions. Hence, the comparison using same Krishna et al, 2021 has been presented in different global ocean region locations derived with OCM-3 GAC and Modis-Aqua datasets and the trend observed to be matching well.

6. Limitations:

The validation of satellite-derived sea surface POC data requires in-situ observations from various types of water bodies and across different seasons to ensure comprehensive accuracy assessment. However, the availability of in-situ validation data remains a challenge and carried out with limited numbers.

Furthermore, achieving validation with cloud-free satellite data poses a significant limitation, particularly during specific seasons when cloud cover is more prevalent. This constraint affects the consistency and reliability of the validation process.

7. Future Aspect:

- Future plans include to validate OCM-3 POC product and fine tune the algorithm.
- This will include organizing more cruises equipped with on-board radiometers to collect in-situ data, including particulate organic carbon (POC) measurements. Expanding the data to validation across different water types and seasons, thereby improving the accuracy.

- Furthermore, inter-sensor comparisons involving data from a wider range of satellite sensors are necessary. These comparisons will help identify and address sensor-specific biases, ensuring greater consistency.
- To develop the POC empirical algorithm for entire Arabian and Bay of Bengal Sea region and fine tuning of different Rrs bands.
- Refinement of the present MBRI algorithm for estimating POC in coastal and Open Ocean waters of the global region with more data points and expansion to global oceans.

8. REFERENCES

1. Allison, D. B., Stramski, D., & Mitchell, B. G. (2010). Seasonal and interannual variability of particulate organic carbon within the Southern Ocean from satellite ocean color observations. Journal of Geophysical Research: Oceans, 115(6), C06002. https://doi.org/10.1029/2009JC005347
2. CEOS, (2014). Strategy for Carbon Observations from Space. The Committee on Earth Observation Satellites (CEOS) Response to the Group on Earth Observations (GEO) Carbon Strategy. *Printed in Japan by JAXA and I&A Corporation*.
3. Chauhan P, Mohan M, Sarangi RK, Kumari B, Nayak S, Matondkar SGP (2002). Surface chlorophyll a estimation in the Arabian Sea using IRS-P4 Ocean Colour Monitor (OCM) satellite data. Int J Remote Sens 23(8):1663–1676.
4. Dall'Olmo, G., Westberry, T., Behrenfeld, M. J., Boss, E., & Slade, W. (2009). Significant contribution of large particles to optical backscattering in the open ocean. *Biogeosciences*, 6, 947–967. doi: 10.5194/bg-6-947-2009
5. Dev, P, J, and Shanmugam, P., (2017). New theoretical formulation for the determination of radiance transmittance at the water-air interface.) OPTICS EXPRESS 27086. Vol. 25(22). https://doi.org/10.1364/OE.25.027086
6. Dev, P, J, and Shanmugam, P.,(2016). Determination of immersion factors for radiance sensors in marine and inland waters: A semi-analytical approach using refractive index approximation. Remote Sensing of the Oceans and Inland Waters: Techniques, Applications, and Challenges, edited by Robert J. Frouin, Satheesh C. Shenoi, K. H. Rao, Proc. of SPIE Vol. 9878, 987803· doi: 10.1117/12.2223711
7. Ducklow, H., Steinberg, D. K., & Buesseler, K. O. (2001). Upper ocean carbon export and the biological pump. *Oceanography*, 14, 50–58. doi: 10.5670/oceanog.2001.06
8. Eppley, R.W., and B.J. Peterson, (1979). Particulate organic matter flux and planktonic new production in the deep ocean. *Nature,* 282(5740): 677-680.
9. Gardner, W., Mishonov, A., & Richardson, M. J. (2006). Global POC concentrations from *in situ* and satellite data. *Deep Sea Research II*, 53, 718–740. doi: 10.1016/j.dsr2.2006.01.029
10. Gower, J. F. R., Doerffer, R., & Borstad, G. A. (1999). Interpretation of the 685nm peak in water-leaving radiance spectra in terms of fluorescence, absorption and scattering, and its observation by MERIS. International Journal of Remote Sensing, 20(9), 1771–1786. https://doi.org/10.1080/014311699212470
11. Hu, S. B., Cao, W. X., Wang, G. F., Xu, Z. T., Lin, J. F., Zhao, W. J., … Yao, L. J. (2016). Comparison of MERIS, MODIS, SeaWiFS-derived particulate organic carbon, and in situ measurements in the South China Sea. International Journal of Remote Sensing, 37(7), 1585–1600. https://doi.org/10.1080/01431161.2015.1088673
12. Joshi, I. D., Stramski, D., Reynolds, R. A., & Robinson, D. H. (2023). Performance assessment and validation of ocean color sensor-specific algorithms for estimating the concentration of particulate organic carbon in oceanic surface waters from satellite observations. Remote Sensing of Environment, 286(May 2022), 113417. https://doi.org/10.1016/j.rse.2022.113417

13. Kharbush, J. J., Close, H.G., Van Mooy, B. A. S., Arnosti, C., Smittenberg, R.H., Le Moigne, F. A. C., Mollenhauer, G., Scholz-Bottcher, B., Obreht, I., Koch, B.P., Becker, K.W., Iversen, M.H., & Mohr, W. (2020). Particulate organic carbon deconstructed: molecular and chemical composition of particulate organic carbon in the Ocean. *Frontiers in Marine Science*, 7:518. doi: 10.3389/fmars.2020.00518
14. King, E. H., Martinez-Vicente, V., Brewin, R.J.W., Dall'Olmo, G., Hickman, A.E., Jackson, T., Kostadinov, T.S., Krasemann, H., Loisel, H., Rottgers, R., Roy, S., Stramski, D., Thomalla, S., Platt, T., & Sathyendranath, S. (2017). Validation and intercomparison of Ocean color algorithms for estimating particulate organic carbon in the Oceans. *Frontiers in Marine Science*, 4:251. doi: 10.3389/fmars.2017.00251
15. Krishna, K. V., Shanmugam, P. & Sarangi, R. K., (2023). Robust algorithm based on the reflectance curvature for estimating particulate organic carbon and its spatiotemporal variability in the global Ocean. *IEEE Transactions on Geoscience and Remote Sensing*, 61, 1-16, doi: 10.1109/TGRS.2023.3304321.
16. Le, C., Lehrter, J. C., Hu, C., MacIntyre, H., & Beck, M. W. (2017). Satellite observation of particulate organic carbon dynamics on the Louisiana continental shelf. *Journal of Geophysical Research Oceans*, 122, 555–569, doi:10.1002/ 2016JC012275
17. Le, C., Zhou, X., Hu, C., Lee, Z., Li, L., & Stramski, D. (2018). A color-index-based empirical algorithm for determining particulate organic carbon concentration in the ocean from satellite observations. *Journal of Geophysical Research Oceans*, 123, 7407–7419.
18. Lee, D., Son, S., Joo, H., Kim. K., Kim, M.J., Jang, H.K., Yun, M.S., Kang, C.K., & Lee, S. H. (2020). Estimation of the particulate organic carbon to chlorophyll-a ratio using MODIS-Aqua in the East/Japan Sea, South Korea. *Remote Sensing*, 12(5):840. https://doi.org/10.3390/rs12050840
19. Li, Q., Jiang, L., Chen, Y., Tang, J., & Gao, S. (2023). Absorption based algorithm for satellite estimating the particulate organic carbon concentration in the global surface ocean. *Frontiers in Marine Science*, 9:1048893. doi: 10.3389/fmars.2022.1048893
20. Lima, I. D., Lam, P. J., and Doney, S. C.: Dynamics of particulate organic carbon flux in a global ocean model, Biogeosciences, 11, 1177–1198, https://doi.org/10.5194/bg-11-1177-2014, 2014.
21. Liu, D., Pan, D., Bai, Y., He, X., Wang, D., Wei, J.-A., & Zhang, L. (2015). Remote Sensing Observation of Particulate Organic Carbon in the Pearl River Estuary. Remote Sensing, 7(7), 8683–8704. https://doi.org/10.3390/rs70708683
22. Longhurst, A. R., and W. G. Harrison (1989). The biological pump: Profiles of plankton production and consumption in the upper ocean, Prog. Oceanogr., 22, 47–123.
23. Parsons, T.R., Maita, C.M., & Lalli, C.M. (1984). A Manual of Chemical & Biological Methods for Seawater Analysis; *Pergamon Press*: New York, NY, USA,
24. Kandasamy, P., Sarangi, R.K., Ayyappan, S., Allimuthu, D., Ramalingam, S., and Durairaj, P., (2019). Influence of sea surface temperature and chlorophyll-a on the distribution of particulate organic carbon in the southwest Bay of Bengal. J. Geomatics 13, 291–303.
25. Prosoft 7.7 Product Manual, Seabird Scientific, SAT-DN-00228, 2017.
26. Sahay, A., A. Gupta, G. Motwani, M. Raman, S. M. Ali, M. Shah, S. Chander, P. R. Muduli, and R. N. Samal. (2019). "Distribution of Coloured Dissolved and Detrital Organic Matter in Optically Complex Waters of Chilika Lagoon, Odisha, India, Using Hyperspectral Data of AVIRIS-NG." Current Science 116 (7): 1166–1171. doi:10.18520/cs/v116/i7/1166-1171.
27. Sarangi R.K., Jaiganesh, S. N. N., Bimalkumar, R., Apurva, P., & Hitesh, D.P. (2023). Particulate Organic Carbon (POC) Estimation and Algorithm Development in Northeast AS Coastal Water. *Thalassas: An International Journal of Marine Sciences*, 39 (2): 621-630.

28. Sarangi RK, Jaiganesh SNN, Raman M (2022). In situ biogeochemical and radiometer based optical parameters observation in Diu coastal water. Tech Rep EPSA/BPSG/MED/TR28
29. Sarangi RK, Singh S, Dwivedi RM, Matondkar SGP (2008). Hyperspectral radiometric observation of the northeast Arabian Sea during April 2006. J Indian Soc Remote Sens (JISRS) 36:13–25
30. Singh, R. K., & Shanmugam, P. (2016). A Multidisciplinary Remote Sensing Ocean Color Sensor: Analysis of User Needs and Recommendations for Future Developments. IEEE Journal of Selected Topics in Applied Earth Observations and Remote Sensing, 9(11), 5223–5238. https://doi.org/10.1109/JSTARS.2016.2520501
31. Singh, R. K., Shanmugam, P., He, X., & Schroeder, T. (2019). UV-NIR approach with non-zero water-leaving radiance approximation for atmospheric correction of satellite imagery in inland and coastal zones. Optics Express, 27(16), A1118. https://doi.org/10.1364/OE.27.0A1118
32. Stramska, M. (2009). Particulate organic carbon in the global ocean derived from SeaWiFS ocean color. Deep Sea Research Part I: Oceanographic Research Papers, 56(9), 1459–1470. https://doi.org/10.1016/j.dsr.2009.04.009
33. Stramski ,D., Joshi,I., Reynolds R.A. (2022). Ocean color algorithms to estimate the concentration of particulate organic carbon in surface waters of the global ocean in support of a long-term data record from multiple satellite missions. Remote Sensing of Environment 269: 112776 https://doi.org/10.1016/j.rse.2021.112776
34. Stramski, D., Reynolds, R. A., Babin, M., Kaczmarek, S., Lewis, M. R., Röttgers, R., … Claustre, H. (2008). Relationships between the surface concentration of particulate organic carbon and optical properties in the eastern South Pacific and eastern Atlantic Oceans. Biogeosciences, 5(1), 171–201. https://doi.org/10.5194/bg-5-171-2008
35. Tilstone, G., Dall'Olmo, G., Hieronymi, M., Ruddick, K., Beck, M., Ligi, M., Costa, M., D'Alimonte, D., Vellucci, V., Vansteenwegen, D., Bracher, A., Wiegmann, S., Kuusk, J., Vabson, V., Ansko, I., Vendt, R., Donlon, C., & Casal, T. (2020). Field Intercomparison of Radiometer Measurements for Ocean Colour Validation. Remote Sensing, 12(10), 1587. https://doi.org/10.3390/rs12101587
36. Tran, T. K., Duforet-Gaurier, L., Vantrepotte, V., Jorge, D. S. F., Meriaux, X., Cauvin, A., et al. (2019). Deriving particulate organic carbon in coastal waters from remote sensing: Inter-comparison exercise and development of a maximum band ratio approach. *Remote Sensing*, 11 (23), 2849. doi: 10.3390/rs11232849
37. Varunan, T., & Shanmugam, P. (2017). An optical tool for quantitative assessment of phycocyanin pigment concentration in cyanobacterial blooms within inland and marine environments. Journal of Great Lakes Research, 43(1), 32–49. https://doi.org/10.1016/j.jglr.2016.11.001
38. Verma, N., Lohrenz, S., Chakraborty, S., Fichot, C.G. (2021). Underway Hyperspectral Bio-Optical Assessments of Phytoplankton Size Classes in the River-Influenced Northern Gulf of Mexico. Remote Sens. 13, 3346. https://doi.org/ 10.3390/rs13173346
39. Volk, T., & Hoffert, M. I. (1985). Ocean carbon pumps: analysis of relative strengths and efficiencies in ocean-driven atmospheric CO_2 changes. In E. T. Sundquist, & W. S. Broecker (Eds.), The carbon cycle and atmospheric CO_2: natural variations Archean to present. Chapman conference papers, 1984 (99-110). *American Geophysical Union*, Geophysical Monograph 32
40. Woźniak, S. B., Darecki, M., Zabłocka, M., Burska, D., & Dera, J. (2016). New simple statistical formulas for estimating surface concentrations of suspended particulate matter (SPM) and

particulate organic carbon (POC) from remote-sensing reflectance in the southern Baltic Sea. Oceanologia, 58(3), 161–175. https://doi.org/10.1016/j.oceano.2016.03.002

41. Wu, H., Cui, L., Wang, L., Sun, R., & Zheng, Z. (2023). A method for estimating particulate organic carbon at the sea surface based on geo-detector and machine learning. *Frontiers in Marine Science*, 10:1295874. doi: 10.3389/fmars.2023.1295874
42. Xing, X.-G., Zhao, D.-Z., Liu, Y.-G., Yang, J.-H., Xiu, P., & Wang, L. (2007). An overview of remote sensing of chlorophyll fluorescence. Ocean Science Journal, 42(1), 49–59. https://doi.org/10.1007/BF03020910